Mon. Not. R. Astron. Soc. **000**, 000–000 (0000) Printed 8 August 2011 (MN LATEX style file v2.2)

A new model for infrared and submillimetre counts

Michael Rowan-Robinson
Astrophysics Group, Blackett Laboratory, Imperial College of Science Technology and Medicine, Prince Consort Road, London SW7 2AZ

arXiv:0812.2609v2 [astro-ph] 20 Dec 2008

8 August 2011

ABSTRACT

A new model for source counts from 8-1100 μm is presented, which agrees well with source-count data and the observed background spectrum. The model is similar to that of Rowan-Robinson (2001), but with different evolution for each of the four assumed infrared template types. The evolution is modified in two ways; (i) the exponential factor is modified so that it tends to a constant value at late times, (ii) the power-law factor is modified so that it tends to zero at redshift z_f, rather than 0 as assumed by Rowan-Robinson (2001). I find strong evidence from the 850 and 1100 μm counts, and from the infrared background, that z_f = 4-5, with some preference for a value at the low end of the range, implying that star-forming galaxies at z > 5 are not significant infrared emitters, presumably due to a low opacity in dust at these early epochs.

The model involves zero or even negative evolution for starbursts and AGN at low redshifts (<0.2), suggesting that the era of major mergers and strong galaxy-galaxy interactions is over.

Key words: infrared: galaxies - galaxies: evolution - star:formation - galaxies: starburst - cosmology: observations

1 INTRODUCTION

Source-counts at infrared and submillimetre wavelengths, combined with the spectrum of the infrared background, give us important constraints on the star-formation history of the universe. First indications of strong evolution in the properties of star-forming galaxies came from IRAS 60 μm counts (Hacking and Houck 1987, Lonsdale et al 1990, Rowan-Robinson et al 1991, Franceschini et al 1991, 1994, Pearson and Rowan-Robinson 1996)

ISO gave us deep counts at 15 μm providing strong evidence for evolution (Oliver et al 1997, Rowan-Robinson et al 1997, Guiderdoni et al 1998, Aussel et al 1999, Elbaz et al 1999, 2002, Serjeant et al 2000, Gruppioni et al 2002, Lagache et al 2003) and useful counts at 90 and 175 μm (Kawara et al 1998, Dole et al 2001, Efstathiou et al 2000a, Heraudeau et al 2004).

850 μm counts with SCUBA on JCMT (Smail et al 1997, Hughes et al 1998, Eales et al 1999, 2000, Barger et al 1999, Blain et al 1999, Fox et al 2002, Scott et al 2002, Smail et al 2002, Cowie et al 2002, Webb et al 2003, Borys et al 2004, Coppin et al 2006) have given important insight into the role of cool dust and also strong constraints on the high-redshift evolution of hyperluminous infrared galaxies. Evidence for luminosity evolution of submillimetre galaxies was given by Ivison et al (2002). 1200 μm counts with MAMBO have been reported by Greve et al (2004) and modelled in terms of a strongly evolving population. Recently the AZTEC collaboration have reported differential counts at 1100 μm (Perera et al 2008, Austermann et al 2008), which provide even stronger constraints on high redshift evolution.

The detection of the infrared background with COBE (Puget et al 1996, Fixsen et al 1998, Hauser et al 1998, Lagache et al 1999) provided an important constraint on evolutionary models (Guiderdoni et al 1997, 1998, Franceschini et al 1998, 2001, Dwek et al 1998, Blain et al 1999, Gispert et al 2000, Dole et al 2001, Rowan-Robinson 2001, Chary and Elbaz 2001, Elbaz et al 2002, King and RR 2003, Balland et al 2003, Xu et al 2003, Lagache et al 2003). Dole et al (2006) used stacking analysis on deep *Spitzer* counts at 24, 90 and 160 μm to estimate the integrated back-

© 0000 RAS

ground radiation from sources at these wavelengths. With *Spitzer* we also have deep counts at 8, 24, 70, 160 μm (Fazio et al 2004, Chary et al 2004, Marleau et al 2004, Papovich et al 2004, Dole et al 2004, Le Floch et al 2005, Frayer et al 2006, Shupe et al 2008), with 24 μm providing an especially complete picture of the contribution of individual sources to the infrared background. While some pre-*Spitzer* models were quite successful at 70 and 160 μm, none captured full details of the 24 μm counts. Lagache et al (2004) provided early revised models in the light of the Spitzer data.

Rowan-Robinson (2001) modeled infrared source-counts and background in terms of four types of infrared galaxy: quiescent galaxies in which the infrared radiation (infrared 'cirrus') is emission from interstellar dust illuminated by the general stellar radiation field, starbursts for which M82 is the prototype, more extreme, higher optical depth starbursts with Arp 220 as prototype, and AGN dust tori. The same evolution history, intended to reflect the global star-formation history, was used for each galaxy type. This model was consistent with counts, luminosity functions and colour-luminosity relations from IRAS, counts from ISO and available integral 850 μm counts. However the advent of deep source-count data from *Spitzer* showed that this model, along with other pre-*Spitzer* models, failed, especially at 24 μm.

In this paper I show how the Rowan-Robinson (2001) model has to be modified to achieve consistency with *Spitzer* and other modern data and give predictions for the *Herschel* and *Planck* wave-bands. Some preliminary results were given in Shupe et al (2008).

A cosmological model with $\Lambda = 0.7$, h_0=0.72 has been used throughout.

2 METHODOLOGY

The philosophy is similar to that of Rowan-Robinson (2001), to find a simple analytic form for the evolutionary function, without discontinuities and involving the minimum number of parameters. I retain the same four basic infrared templates: (1) quiescent galaxies, radiating in the infrared through emission by interstellar dust of absorbed starlight (' infrared cirrus'), (2) starbursts, with prototype M82, (3) extreme starbursts with much higher dust optical depth, with prototype Arp 220, (4) AGN dust tori. These templates, which have been derived through radiative transfer calculations (Efstathiou and Rowan-Robinson 1995, 2003, Rowan-Robinson 1995, Efstathiou et al 2000b), have proved extremely effective in modeling the spectral energy distributions (SEDs) of infrared galaxies in the ISO-ELAIS (Rowan-Robinson et al 2004), *Spitzer*-SWIRE (Rowan-Robinson et al 2005) and SHADES (Clements et al 2008) surveys . The luminosity functions for each component are derived as in Rowan-Robinson (2001), from the 60 μm luminosity function via a mixture table which is a function of 60 μm luminosity (Figure 1). These luminosity functions are essentially unchanged from Rowan-Robinson (2001), except that the Arp 220 component has been assumed to be more significant in the luminosity range $L_{60} = 10^9 - 10^{10} L_\odot$, in order to improve the fit to the counts at 850 μm (see below).

Table 1. Evolutionary parameters for each component

component	P	Q	a_0
cirrus	4.0	10.0	0.6
M82	2.7	18.0	0.994
A220	2.7	13.6	0.92
AGN	2.7	13.0	0.94

The main new feature of the current work is that I now allow each component its own evolution function, since a single evolution function for all components is not capable of reproducing the latest counts, especially at 24 μm.

In Rowan-Robinson (2001) I assumed a pure luminosity evolution, with $L(z) = \phi(z)L(0)$, and

$\phi(z) = expQ(t_0 - t)/t_0(t/t_0)^P$ (1)

where t_0 is the current epoch, the exponential factor is essentially the Bruzual and Charlot (1993) star-formation history and the power law factor ensures that L(z) tends to zero as t tends to 0. Thus t_0/Q has the meaning of the exponential time-scale for star-formation. The peak star-formation rate in this model occurs at $t/t_0 = P/Q$.

However the 24 μm counts show an extended Euclidean behaviour at bright fluxes and I have therefore allowed for the possibility that the evolution function tends asymptotically to a constant value at late times. I also allow the epoch where the evolution function tends to zero at early times to be $t_f = t(z_f)$ rather than zero, where z_f is to be determined from the fits to the counts. This option was found to be important at submillimetre wavelengths. Thus I assume

$\phi(z) = [a_0 + (1 - a_0)expQ(1 - y)](y^P - (y_f)^P)$ (2)

where $y = (t/t_0)$, $y_f = t(z_f)/t_0$.

The strategy for determining the parameters P, Q, a_0 for each component was as follows. First we allowed all parameters to vary while seeking a best-fit solution to the 24 μm counts. This fixed the parameters for the cirrus and M82 components. Keeping these fixed we set P for the AGN dust tori to have the same value as the M82 starburst component and then optimized Q and a_0 for the dust tori to fit the 24 μm counts, while requiring that the proportion of dust tori dominated sources at S(24) = 1 mJy be no less than 20 %, based on analysis of the SWIRE survey (Rowan-Robinson et al 2005). These parameter choices essentially then determined, without further adjustment, the counts at 8, 15, 70 and 160 μm and the goodness of fit at these wavelengths is a test of

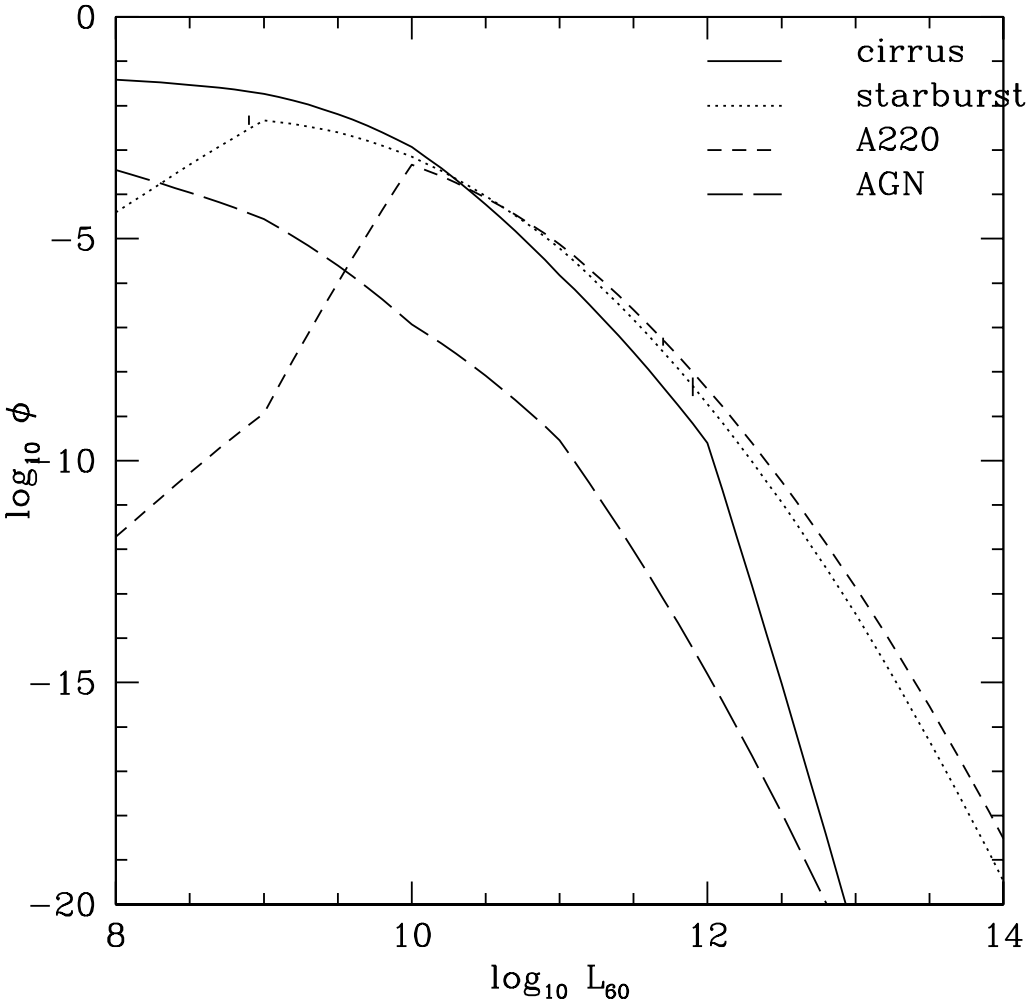

Figure 1. Contributions to 60 μm luminosity function of cirrus (solid), M82 (dotted), A220 (dashed), and AGN dust tori (long-dashed) infrared components.

the broad physical validity of the assumed template and luminosity function.

The predicted counts at 850 (and 1100) μm depend sensitively on the evolutionary parameters for Arp 220 starburst component, but these parameters are essentially undetermined at 24 μm. It became clear that the proposal of Efstathiou and Rowan-Robinson (2003) that cirrus galaxies could make a dominant contribution at S(850) = 8 mJy, was not consistent with the count model approach adopted here, although they do become dominant at S(850) < 1 mJy in these count models. The evolutionary parameters for the A220 component were adjusted to give an equal contribution of A220 and M82 starbursts at S(850) = 8 mJy, since SED modelling of SHADES sources (Clements et al 2008) suggests both templates are important at these fluxes . This also required an increase in the luminosity function for A220 sources at lower luminosities. We are not able to reduce the contribution of M82 starbursts in the submm without destroying the fit to the counts at 8-160 μm. Evidence that submillimetre sources do not constitute a monolithic, Arp-220-like, population has been given by Menendez-Delmestre et al (2007), Ibar et al (2008 and Pope et al (2008).

Adopted values of P, Q, a_0 for each of the four components are given in Table 1. Figure 2 shows the adopted evolution functions for the four infrared components, with values of z_f of 4, 5 and 10 illustrated. The model suggests zero or even negative evolution for some components at low redshifts and it would be interesting to test this with large area far infrared surveys. The physical interpretation would be that the era of major mergers and strong interactions is over, with the remaining star-formation at the present

epoch being relatively quiescent or driven by weaker interactions.

I should emphasize that the assumed evolution is applied to all infrared luminosities, and I find no need to postulate very strong evolution only of luminous galaxies as has been proposed in many source-count models in the literature.

The assumption of a pure luminosity evolution is perhaps questionable, since we know that galaxies grow by mergers, so that we expect some positive density evolution with redshift for more massive galaxies and negative evolution for lower masses. However the evolution we are trying to describe in eqn (2) refers only to star-forming, dusty galaxies. If mergers involve fragments which are not star-forming or have little dust, they will not contribute to density evolution at these wavelengths. It would be desirable in future work to relate evolutionary models to semi-analytical models for the merger of dark matter halos and the subsequent evolution of star-formation and dust, but this is beyond the scope of the present paper.

3 FITS TO COUNTS

Here I discuss the fits to counts at 8-1100 μm. The most challenging wavelength is 24 μm, with a relatively Euclidean behaviour at bright fluxes, a very sharp steepening of the counts between 3 mJy and 300 μJy, and a strong flattening of the source-count slope fainter than 200 μJy. Figure 3 shows my fit to the *Spitzer* 24 μm differential (Euclidean-normalized) counts, indicating the contribution of each of the four infrared spectral types. Both cirrus and M82 starbursts are important at bright fluxes, but the strong steepening of the counts is attributed solely to M82 starbursts. AGN dust tori make their strongest contribution at 1-10 mJy. Arp220 starburst make only a small contribution at all fluxes.

The 15 μm predicted differential counts (Fig 4R) fitted to ISO data show similar characteristics to the 24 μm counts but the interpretation is quite different with cirrus galaxies dominant at all fluxes. This reflects the strong difference between the spectral energy distributions (SEDs) of cirrus and M82 templates in the mid infrared. The 8 μm predicted differential counts are compared to Spitzer data (Fazio et al 2006) in Fig 4L. These appear quite different from the 15 and 24 μm counts, because they are far more strongly dominated by quiescent galaxies.

Figure 5 shows the fit to *Spitzer* counts at 70 and 160 μm differential counts. Here we see dominance by cirrus galaxies at bright fluxes and M82 starbursts at faint fluxes

Figure 6L shows the fit to SCUBA differential counts at 850 μm (Coppin et al 2006). Cirrus galaxies are predicted to dominate at the very highest fluxes, though we have no source-count information at these fluxes yet. The *Planck* mission should remedy this. At the fainter fluxes sampled by SCUBA surveys I predict that Arp220 starbursts should dominate above 10 mJy and M82 starbursts below this. This is consistent with the SED modelling of SHADES sources by Clements et al (2008), which shows both templates being needed to fit the multiwavelength SEDs. There is a strong dependence on the redshift at which infrared starbursts are assumed to switch on, z_f, with values in the range 4 to 5 favoured by 850 μm counts.

Figure 6R shows the fit to the GOODS 1100 μm differential counts (Perera et al 2008). These are similar to the 850 μm counts in interpretation, with z_f = 4-5 again being favoured. This is at first sight surprising since there is clear evidence now of galaxies at redshifts 6-7. However it is consistent with the 850 μm spectroscopic redshift compilation of Chapman et al (2003, 2005), which shows no redshifts > 4. That work was subject to the constraint that the 850 μm sources be detected at radio wavelengths and this could affect the ability to detect high redshift objects, but Chapman et al (2005) argue that this is not a major selection effect and that no more than 10 % of the submillimetre population could be at z > 4. A few individual submillimetre galaxies have been found at z > 4 (Wang et al 2007, Younger et al 2007, Schinnerer et al 2008), but there does not appear to be a large population of z > 4 submillimetre galaxies. The negative K-correction operating at submillimetre wavelengths (Franceschini et al 1991, Blain and Longair 1993) means that dust-emitting galaxies of redshift 7 should have been clearly detectable in 850 μm surveys. Presumably the low metallicity at early times means star-forming regions are not opaque to dust so star-forming galaxies at z = 5-7 emit purely in the optical and ultraviolet.

The models are also consistent with the MAMBO 1200 μm integral counts of Greve et al (2004), but integral counts do not strongly constrain model parameters because of the non-independence of the errors. *Herschel* and *Planck* submillimetre counts will provide much stronger tests of these models.

Figure 7 shows a composite plot of differential counts at 8-1100 μm, each wavelength horizontally displaced for clarity. Predictions for all these wavelengths (and others of interest for *Akari*, *Herschel* and *Planck*) are available at http://astro.ic.ac.uk/ ∼mrr/counts

4 INFRARED BACKGROUND

The infrared background spectrum provides a strong test of the assumed evolution and SEDs. Figure 8 shows the fit of my best counts model to the infrared background spectrum, showing the effect of assuming z_f = 4, 5, 10. The 100-850 μm background measurements require z_f = 4-5, with 4 giving the best fit.

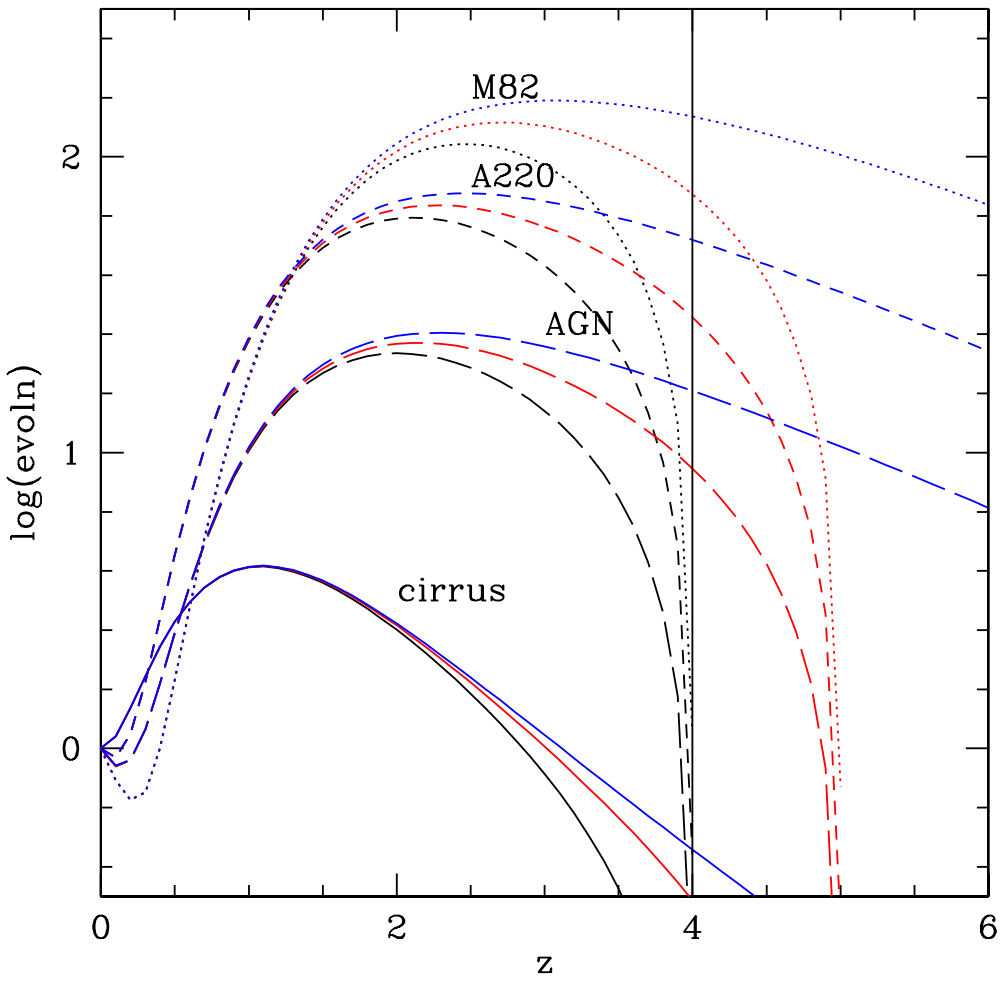

Figure 2. Evolution rate for cirrus (solid), M82 (dotted), A220 (dashed), and AGN dust tori (long-dashed) infrared components. Black curves: adopted maximum redshift of 4; red curves: maximum redshift 5; blue curves: maximum redshift 10.

So both the background spectrum and the 1100 μm counts are both sensitive to z_f and require z_f = 4-5.

The fit to the background spectrum from 15-850 μm is excellent. In Fig 8 I have shown the relative contribution of the different infrared poulations, with cirrus galaxies dominating at 8-24 μm, M82 starbursts dominating to 100 μm, and then cirrus galaxies again dominating in the submillimetre, by virtue of their dominance of the very faint source counts. The Arp220, high optical depth, starbursts, which are the dominant contribution to the infrared luminosity function above $10^{12} L_{\odot}$, contribute only about 10% of the submillimetre background. AGN dust tori contribute about 0.5 % of the mid infrared background and a negligible fraction of the submillimetre background.

5 PREDICTED REDSHIFT DISTRIBUTIONS

Detailed predictions of the models are given at a wide range of wavelenghs from 8-1100 μm, including the survey wavelengths of Planck and Herschel (astro.ic.ac.uk/ ∼mrr/counts/). These include the redshift distribution for each infrared type at each flux.

Figure 9 illustrates redshift distributions at 200 μJy at 24 μm and at 5 mJy at 850 μm. The 850 μm distribution agrees rather well with the Chapman et al (2003, 2005) measured distribution. The predicted 24 μm distribution shows far more z > 1 sources than in the distribution derived by Rowan-Robinson et al (2008) from their SWIRE photometric redshift catalogue, reflecting the rather shallow optical photometry for most of that catalogue.

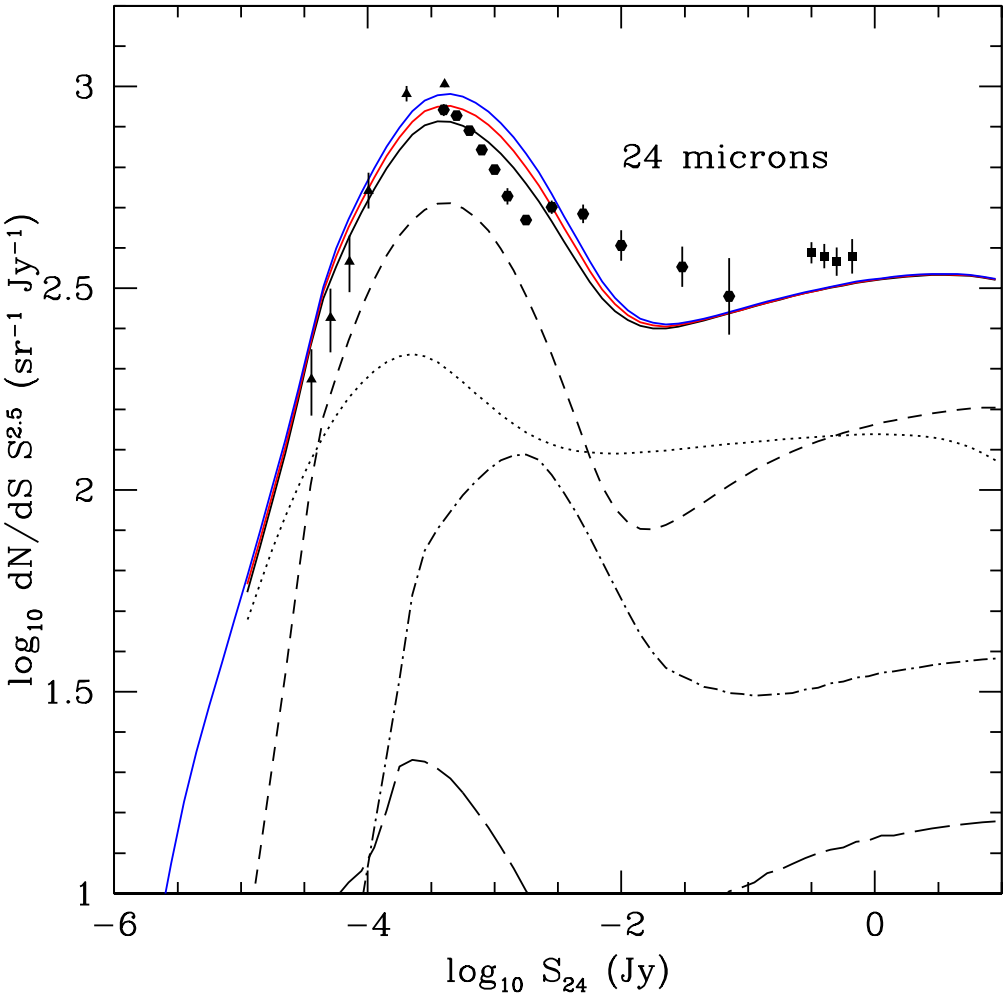

Figure 3. Euclidean normalised differential counts 24 μm. Solid curve: total counts (black: $z_f = 4$, red(upper): $z_f = 5$) ; dotted curve: cirrus; short-dashed curve: M82; long-dashed curve: A220; dash-dotted curve: and AGN dust tori. Black curves: maximum redshift 4; red curve: maximum redshift 5, blue curve: maximum redshift 10. Filled circles: SWIRE data from Shupe et al (2008), triangles: data from Papovich et al (2004).

6 DISCUSSION

The model presented here, based on four basic infrared templates is obviously an oversimplification. We know that to understand local galaxies we need a range of cirrus components (Rowan-Robinson 1992, Efstathiou and Rowan-Robinson 2003). From the models of Efstathiou et al (2000) the SED of a starburst varies strongly with the age of the starburst so the representation as two simple extremes, M82 and Arp220 starbursts, is oversimplified. Finally we know that we need a range of dust torus models to fit ultraluminous and hyperluminous galaxies (Efstathiou and Rowan-Robinson 1995, Rowan-Robinson 2000, Farrah et al 2003).

However the four templates used here do capture the main features of the infrared galaxy population. In fitting the SEDs of ISO and *Spitzer* sources (Rowan-Robinson et al 2004, 2005, 2008), we allow individual sources to include cirrus, M82 or Arp220 starburst, and an AGN dust torus, which gives a rich range of predicted SEDs. This works for SCUBA sources (Clements et al 2008) and for detailed IRS spectroscopy of infrared galaxies (Farrah et al 2008).

The strongest evolution rate is found for M82 starbursts. Arp220 starburst peak at a slightly later redshift (2 rather than 2.5) and at a slightly lower amplitude. AGN dust tori, where the evolution reflects the accretion history, also peak at redshift 2, but show a less steep decline to the present than M82 or Arp220 starbursts, suggesting a gradual change in the relative efficiency with which gas is converted to stars or accreted into a central black hole.

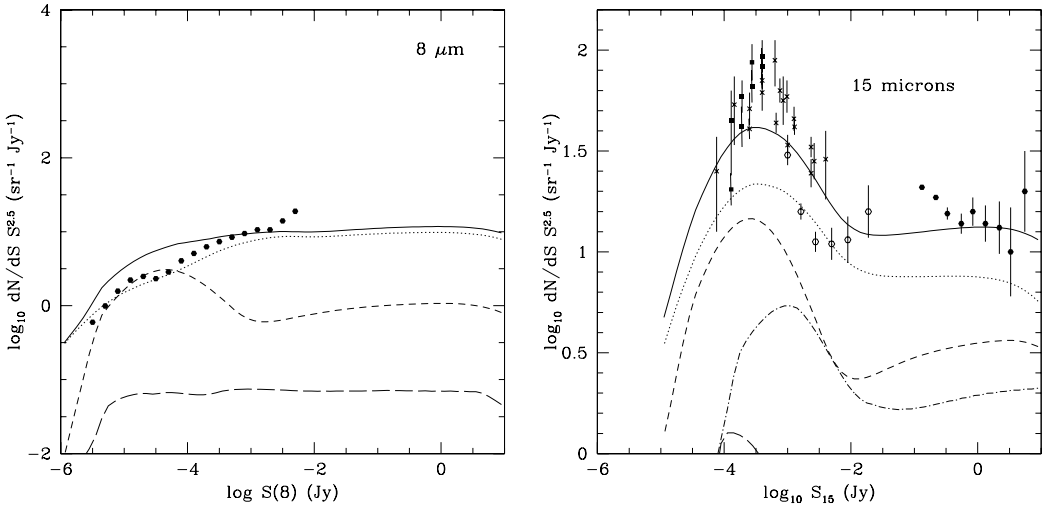

Figure 4. Euclidean normalised differential counts at 8 (LH) (data from Fazio et al 2004) and 15 (RH) μm (ISO data from Elbaz et al 1999 (open triangles), Aussel et al 1999 (filled triangles), Gruppioni et al 2002 (open circles); interpolated IRAS data (filled circles) from Verma (private communication). Solid curve: total counts; dotted curve: cirrus; short-dashed curve: M82; long-dashed curve: A220; dash-dotted curve: AGN dust tori.

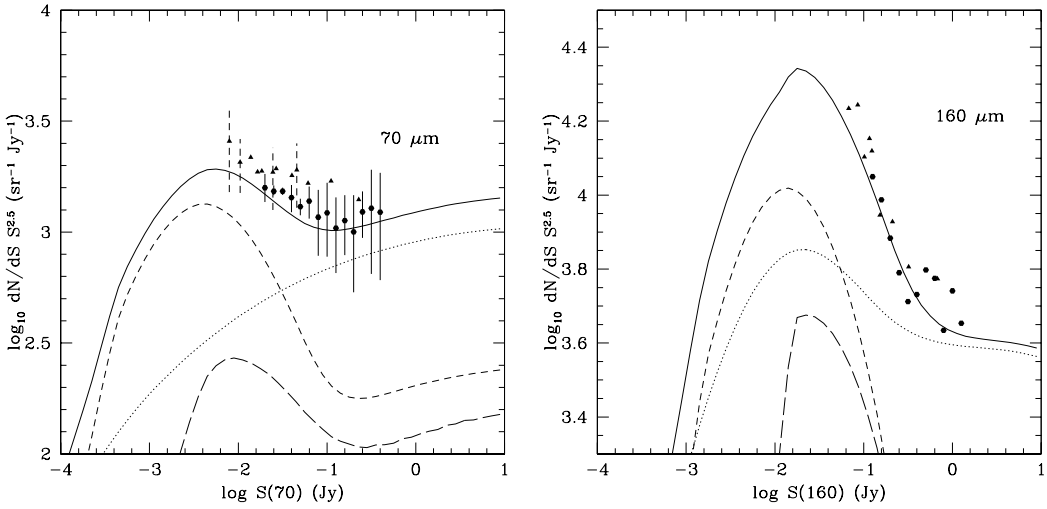

Figure 5. Euclidean normalised differential counts at 70 (LH) and 160 (RH) μm (filled circles: SWIRE Afonso-Luis et al (2008 in preparation), triangles: FLS Frayer et al 2006) . Solid curve: total counts; dotted curve: cirrus; short-dashed curve: M82; long-dashed curve: A220; dash-dotted curve: AGN dust tori. Black curves: maximum redshift 4; red curve: maximum redshift 5.

Cirrus galaxies show a much more modest evolution rate, peaking at redshift 1, and with an amplitude only a factor of 3 greater than the present epoch. However even in relatively quiescent galaxies like our own or M81, the star formation activity was greater at redshift 1 than at the present day. This would also imply a higher interstellar medium dust optical depth in spirals at z $\sim$ 1, an effect that may have been detected (Rowan-Robinson 2003, Rowan-Robinson et al 2008).

Lagache et al (2004) modified their 2003 model (Lagache et al 2003) for far infrared counts and the background spectrum with changes to the luminosity-density evolution and to the 2-30 μm SED of their starburst component. Their earlier model involves modest density evolution for normal cirrus galaxies from z = 0 to 0.4, then constant luminosity-density to z = 5, followed by a slow decline to z = 8. For starbursts the luminosity-density rises steeply to z = 0.5, is relatively flat to z = 4, and then declines to redshift 8. Lagache et al (2004) also provide successful fits to counts from 15-850 μm and the background

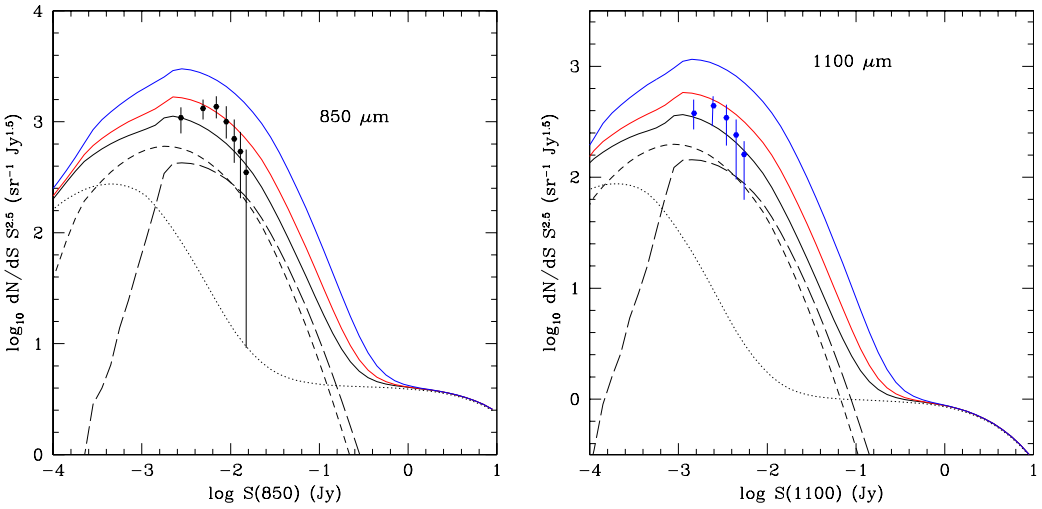

Figure 6. Euclidean normalised differential counts at 850 (LH) (SHADES data from Coppin et al 2006) and 1100 (RH) μm (GOODS data from Perera et al 2008). Solid curve: total counts; dotted curve: cirrus; short-dashed curve: M82; long-dashed curve: A220; dash-dotted curve: AGN dust tori. Black curves: maximum redshift 4; red curve: maximum redshift 5; blue curve: maximum redshift 10.

spectrum, with a philosophy rather different from the present paper. The evolution function involves several discontinuous changes, a feature I have avoided in the present work. I see no necessity to modify our well-tested SED models for starburst galaxies. Abundant *Spitzer*-IRS data supports our assumed templates (eg Farrah et al 2008).

7 CONCLUSIONS

I have presented a new model for source counts from 8-1100 μm, which agrees well with source-count data and the observed background spectrum. The model is similar to that of Rowan-Robinson (2001), but with different evolution for each of the four assumed infrared template types. The evolution is modified in two ways; (i) the exponential factor is modified so that it tends to a constant value at late times, (ii) the power-law factor is modified so that it tends to zero at redshift z_f, rather than 0 as assumed by Rowan-Robinson (2001). I find strong evidence from the 850 and 1100 μm counts and from the infrared background that z_f = 4-5, with some preference for a value at the low end of the range, implying that star-forming galaxies at z > 5 are not significant infrared emitters, presumably due to a low opacity in dust at these early epochs.

The model involves zero or even negative evolution for starbursts and AGN at low redshifts (<0.2), suggesting that the era of major mergers and strong galaxy-galaxy interactions is over.

Herschel and *Planck* submillimetre counts will provide much stronger tests of these models.

8 ACKNOWLEDGEMENTS

I thank the referee for helpful comments which helped me improve the paper.

REFERENCES

Aussel H. et al, 1999, AA351, 37
Austermann J.E., et al, 2008, MNRAS (to be submitted)
Balland C., DevriendtJ.E.G., Silk J., 2003, MNRAS 343, 107
Barger A.J., Cowie L.L., Sanders D.E., 1999, ApJ 518, L5
Borys C., Scott D., Chapman S.C., Halpern M., Nandra K., Pope A., 2004, MNRAS 355, 485
Bruzual A.G., and Charlot, S., 1993, ApJ 405, 538
Blain A.W., Longair M.S., 1993, MNRAS 264, 509
Blain A.W., Smail I., Ivison R.J., Kneib J.-P., 1999, MNRAS 302, 632
Capak P. et al, 2008, ApJ 681, L53
Chapman S.C., Blain A.W., Ivison R.J., Smail I.R., 2003, Nature 422, 695
Chapman S.C., Blain A.W., Ivison R.J., Smail I.R., 2005, ApJ 622, 772
Chary R. and Elbaz D., 2001 ApJ 556, 562
Chary R., Casertano S., Dickenson M.E., Ferguson H.C., Eisenhardt P.R.M., Elabaz D., Grogin N.A., Moustakas L.A., Reach W.T., Yan H., 2004 ApJS 154, 80
Clements D. et al, 2008, MNRAS 387, 247
Coppin K. et al, 2006, MNRAS 372, 1621
Cowie L.L., Barger A.J., Knieb J.-P., 2002, AJ 123, 2197
Dannerbauer H., Walter F., Morrison G., 2008, ApJ 673, L127
Dole H., et al, 2001, AA 372, 364
Dole H. et al, 2004, ApJS 154, 87
Dole H., Lagache G., Puget J.-L., Caputi K.I., Fernandez-Conde N., Le Floc'h C., Papovich C., Perez-Gonzalez P.G., Rieke G.H., Blaylock M., 2006, AA 451, 417

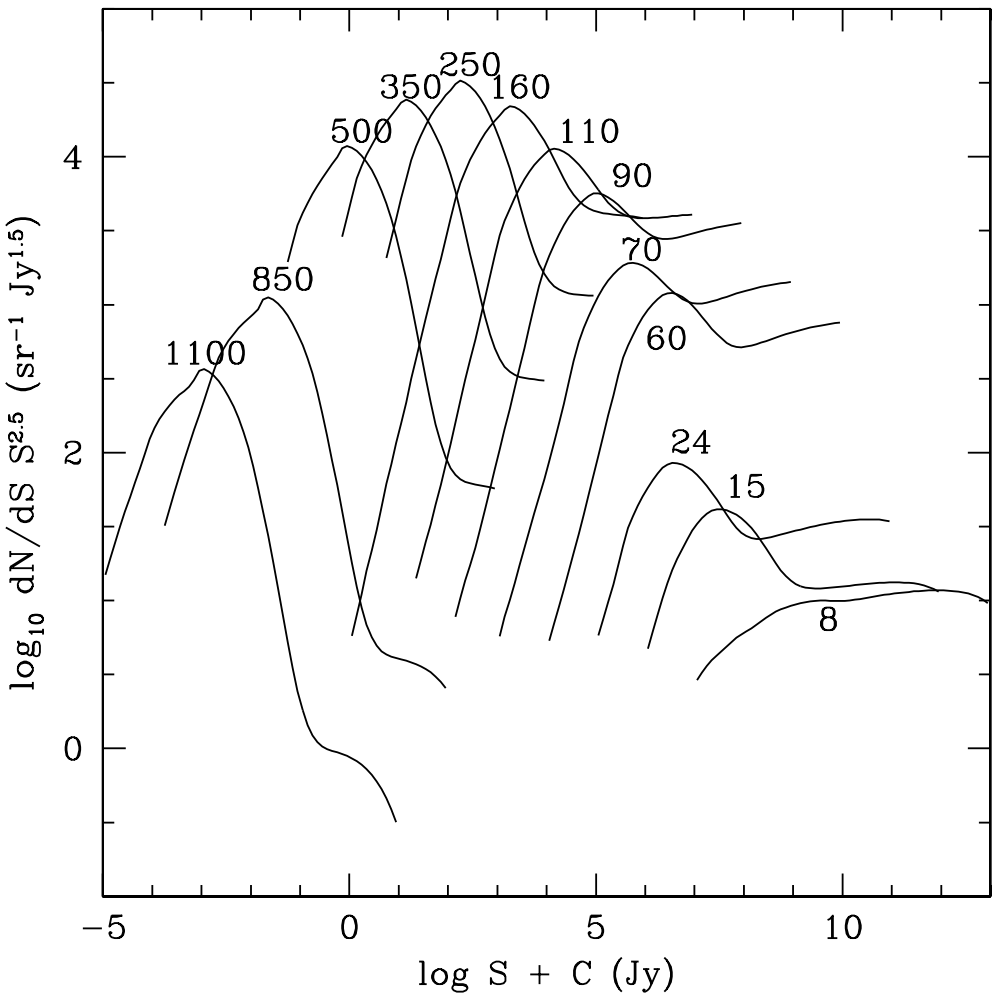

Figure 7. Euclidean normalised differential counts at wavelengths from 8-1100 μm, each displaced by 1 dex for clarity.

Dwek E., Arendt R.G., Hauser M.G., Fixsen D., Kelsall T., Leisawitz D., Pei Y.C., Wright E.L., Mather J.C., Moseley S.H., Odegard N., Shafer R., Silverberg R.F., Weiland J.L., 1998, ApJ 508, 106

Eales S., Lilly S.J., Gear W.K., Dunne L., Bond J.R., Hammer F., Le Fevre O., Crampton D., 1999, ApJ 515, 518

Eales S., Lilly S.J., Webb T., Dunne L., Gear W., Clements D., Yun M., 2000, AJ 120, 2244

Efstathiou A., Rowan-Robinson M., 1995, MNRAS 273, 649

Efstathiou A. et al, 2000a, MNRAS 319, 1169

Efstathiou A., Rowan-Robinson M., Siebenmorgen R., 2000b, MNRAS 313, 734

Efstathiou A., Rowan-Robinson M., 2003, MNRAS 343, 322

Elbaz D. et al, 1999, AA 351, L37

Elbaz D., Cesarsky C.J., Chanial P., Aussel H., Franceschini A., Fadda D., Chary R.R., 2002, AA 384, 848

Farrah D., Afonso J., Efstathiou A., Rowan-Robinson M., Fox M., Clements D., 2003, MNRAS 343, 585

Farrah D., Lonsdale C.J., Weedman D.W., Spoon H.W.W., Rowan-Robinson M., Polletta M., Oliver S., Houck J.R., Smith H.E., 2008, ApJ 677, 957

Fazio G.G. et al, 2004, ApJ 154, 10

Fixsen D.J., Dwek E., Mather J.C., Bennett C.L., Shafer R.A., 1998, ApJ 508, 123

Fox M.J. et al, 2002, MNRAS 331, 839

Franceschini A., Toffolatti L., Mazzei P., Danese L., De Zotti G., 1991, AAS 89, 285

Franceschini A., Mazzei, P., de Zotti, G., Danese, L., 1994, ApJ 427, 140

Franceschini A., Silva L., Fasano G., Granato G.L., Bressan A., Arnouts S., Danese L., 1998, ApJ 506, 600

Franceschini A., Aussel H., Cesarsky C.J., Elbaz D., Fadda D., 2001, AA 378, 1

Frayer D.T., Huynh M.T., Chary R., Dickinson M., Elbaz D., Fadda D., Surace J.A., Teplitz H.I., Yan L., Mobasher B., 2006, ApJ 647, L9

Gispert R., Lagache G., Puget J.-L., 2000, AA 360, 1

Greve T.R., Ivison R.J., Bertoldi F., Stevens J.A., Dunlop J.S., Lutz D., Carilli C.L., 2004, MNRAS 354, 779

Gruppioni C., Lari C., Pozzi F., Zamorani G., Franceschini

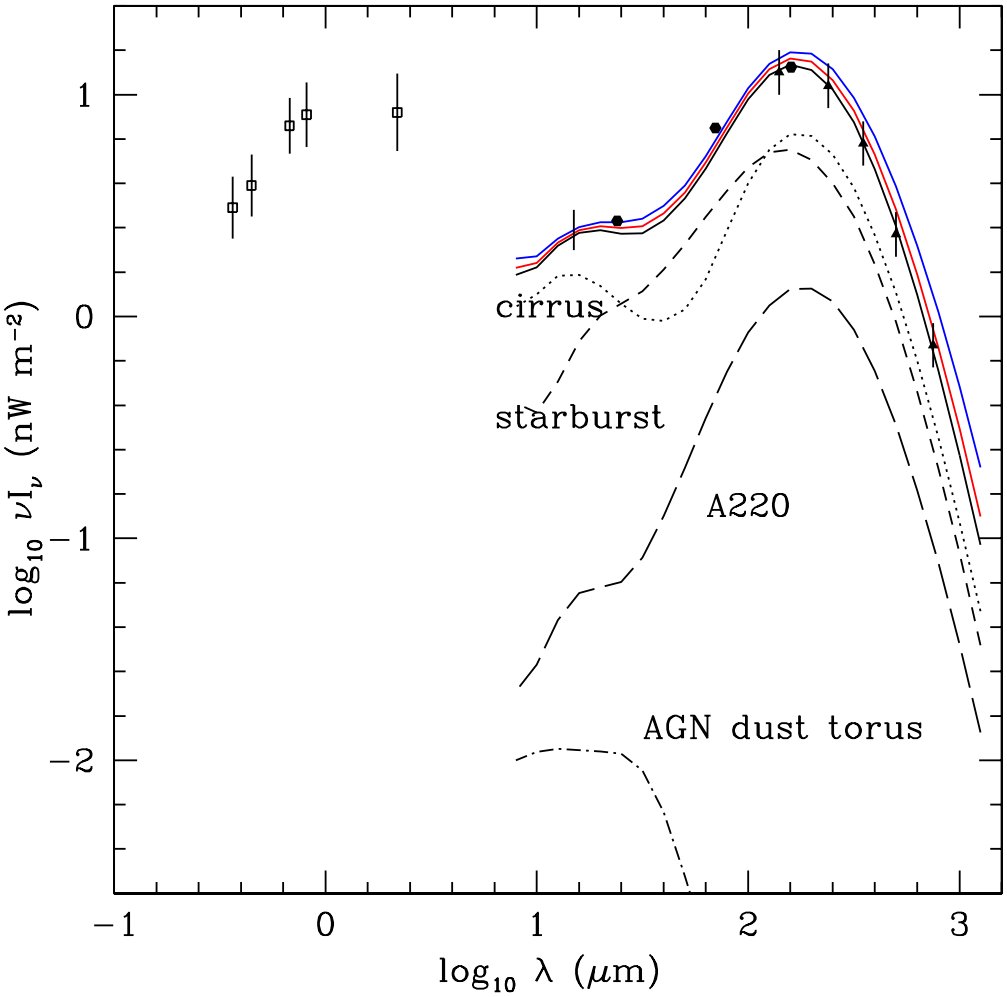

Figure 8. Predicted integrated background spectrum in infrared and submillimetre for maximum redshift 4 (black), 5 (red), 10(blue) showing contribution of different template populations. Data from Fixsen et al (1998, open triangles), Dole et al (2006, filled circles), Serjeant et al (2000, vertical bar), Pozzetti et al (1998, open squares).

A., Oliver S., Rowan-Robinson M., Serjeant S., 2002, MNRAS 335, 831
Guiderdoni B., Bouchet F.R., Puget J.-L., Lagache G., Hivon E., 1997, Nature 390, 257
Guiderdoni B, Hivon E., Bouchet F.R., Maffei B., 1998, MNRAS 295, 877
Hacking P.B. and Houck J., 1987, ApJS 63, 311
Hauser M.G., Arendt R.G., Kelsall T., Dwek E., Odegard N., Weiland J.L., Freudenreich H.T., Reach W.T., Silverberg R.F., Moseley S.H., Pei Y.C., Lubin P., Mather J.C., Shafer R.A., Smoot G.F., Weiss R., Wilkinson D.T., Wright E.L., 1998, ApJ 508, 25
Heradeau Ph., et al, 2004, MNRAS 354, 924
Hughes D.H., Serjeant S., Dunlop J., Rowan-Robinson M., Blain A., Mann R.G., Ivison R., Peacock J., Efstathiou A., Gear W., Oliver S., Lawrence A., Longair M., Goldschmidt P., Jenness T., 1998, Nat 394, 241
Ibar E., Cirasuolo M., Ivison R., Best P., Smail I., Biggs A., Simpson C., Dunlop J., Almaini O., McLure R., Foucaud S., Rawlings S., 2008 MNRAS 386, 953
Ivison R.J., et al, 2002, MN 337, 1
Kawara K., Sato Y., Matsuhara H., Taniguchi Y., Okuda H., Sofue Y., Matsumoto T., Wakamatsu K., Karoji H., Okamura S., Chambers K.C., Cowie L.L., Joseph R.D., and Sanders D.B., 1998, AA 336, L9
King A.J., Rowan-Robinson M., 2003, MNRAS 339, 260
Lagache G., Abergel A., Boulanger F., Desert F.-X., Puget J.-L., 1999, AA 344, 322
Lagache G., Dole H., Puget J.-L., 2003, MNRAS 338, 555
Lagache G., et al, 2004, ApJS 154, 112
Le Floch E. et al, 2005, ApJ 632, 169
Lilly, S.J., Le Fevre, O., Hammer, F., Crampton, D., 1996, ApJ 460, L1
Lonsdale C.J., Hacking P.B., Conrow T.B., Rowan-Robinson M., 1990, ApJ 358, 60
Marleau F.R.l, 2004, ApJS 154, 66
Menendez-Delmestre K., Blain A.W,m Alexander D.M., Smail I., Armus L., Chapman S.C., Frayer D.T., Ivison

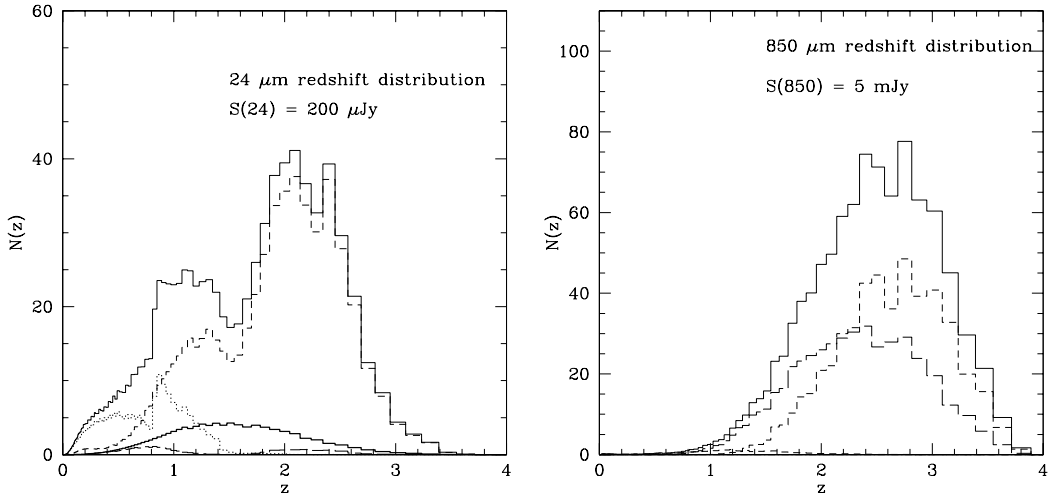

Figure 9. Redshift distribution at 24 μm (LH) and 850 μm (RH), at S(24) = 200 μJy and S(850) = 5 mJy, respectively.

R.,J., Teplitz H.I., 2007, ApJ 655, L65
Oliver S. et al, 1997, MNRAS 289, 471
Papovich C. et al, 2004, ApJS 154, 70
Pearson C., Rowan-Robinson M., 1996, MNRAS 283, 174
Perera T.A., Chapin E.L., Austermann J.E., Scott K.S., Wilson G.W, Halpern M., Pope A., Scott D., Yun M.S., Lowenthal J.D., Morrison G. et al, 2008, MNRAS (in press), astro-ph/0806.3791
Pope A. et al, 2008, ApJ(in press), astro-ph/0808.2816
Pozzetti L., Madau P., Ferguson H.C., Zamorani G., Bruzual G.A., 1998, MNRAS 298, 1133
Puget, J.-L., Abergal A., Bernard J.-P., Boulanger F., Burton W.B., Desert F.-X., Hartmann D., 1996, AA 308, 5
Rowan-Robinson M., Lawrence A., Saunders W., 1991, MNRAS 253, 485
Rowan-Robinson M., 1992, MNRAS 258, 787
Rowan-Robinson M., 1995, MNRAS 272, 737
Rowan-Robinson M. et al, 1997, MNRAS 289, 490
Rowan-Robinson M., 2000, MNRAS 316, 885
Rowan-Robinson M., 2001, ApJ 549, 745
Rowan-Robinson M., 2003, MNRAS 345, 819
Rowan-Robinson M. et al, 2004, MNRAS 351, 1290 129, 1183
Rowan-Robinson M. et al, 2005, AJ 129, 1183
Rowan-Robinson M. et al, 2008, MNRAS 386, 697
Schinnerer E., Carilli C.L., Capak P., Martinez-Sansigre A., Scoville N.Z., Smolcic V., Taniguchi Y., Yun M.S., Bertoldi F., Le Fevre O., de Ravel L., 2008, ApJL (in press), astro-ph/0810.3405
Scott S.E. et al, 2002, MNRAS 331, 817
Serjeant S. et al, 2000, MNRAS 316, 768
Shupe D.L. et al, 2008, AJ 135, 1050
Smail I., Ivison R.J., Blain A.W., 1997, ApJL 490, L5
Smail I., Ivison R.J., Blain A.W., Kneib J.-P., 2002, MNRAS 331, 495
Wang W.H. et al, 2007, ApJ 670, L89
Webb T.M. et al, 2003, ApJ 587, 41
Xu C., Lonsdale C.J., Shupe D.L., Franceschini A., Martin C., Schiminovich D., 2003, ApJ 587, 90
Yoshii Y. and Takahara F., 1988, ApJ 326, 1
Younger J.D. et al, 2007, ApJ 671, 1531